

CFD Analysis of Flow in a Grated Inlet

T. V. Hromadka II¹, P. Rao², Mohsen Battoei³

¹Department of Engineering-Mathematics, United States Military Academy, West Point, NY, USA

²Department of Civil and Environmental Engineering, California State University, Fullerton, CA, USA

³CFD Consultant, Hromadka & Associates, Rancho Santa Margarita, CA, USA

Email: mprasadarao@fullerton.edu

How to cite this paper: Hromadka II, T.V., Rao, P. and Battoei, M. (2020) CFD Analysis of Flow in a Grated Inlet. *Open Journal of Civil Engineering*, **10**, 32-42.
<https://doi.org/10.4236/ojce.2020.101004>

Received: December 24, 2019

Accepted: March 7, 2020

Published: March 10, 2020

Copyright © 2020 by author(s) and Scientific Research Publishing Inc.

This work is licensed under the Creative Commons Attribution International License (CC BY 4.0).

<http://creativecommons.org/licenses/by/4.0/>



Open Access

Abstract

Effectively managing floods in urban regions requires effectively designed and well-maintained runoff collection system. The absence of such a system and intense rainfall event will have the potential to disrupt the urban life and cause significant economic loss to properties. Grated inlets, which are a key component in urban drainage network, are used to capture the runoff. In this work, a three dimensional CFD model was developed based on open-source CFD tool, OpenFOAM[®], to model flow over a grated inlet. An incompressible, transient, multiphase flow, Volume of Fluid (VOF) simulation was performed to predict the water flow rate through the grate inlet. The predicted flow rates are compared with the HEC-22 monograph values. The close agreement between the results shows the potential of using CFD modeling approach to test the reliability of existing drainage inlets for different flow scenarios.

Keywords

Drainage, Grates, Overland Flow, OpenFOAM[®]

1. Introduction

A key constituent of urban drainage infrastructure is the surface runoff collection system. Proper design and maintenance of the components in this collection system can minimize the effect of damage and flooding from a storm event. Such a system will collect the surface runoff, carry the flow through the sewer network, and discharge it to water receiving body. The components in the collection system are 1) street gutters 2) stormwater inlets, and 3) storm sewers. The street gutters collect the runoff from the street and convey it to a storm inlet so that there is no disruption to the traffic on the street. Inlets collect the water from the streets and transit the flow to the sewer network, and provide access for maintaining the storm sewer system. Storm sewers transport the water to a receiving

water body.

The stormwater inlets, also known as Street inlets, are the connecting elements between the surface and the underground sewer system. Street inlets can be four types. These are 1) grate inlets 2) curb-opening inlets 3) combination inlets and 4) slotted drain inlets (Brown *et al.* 2009). Some of the grate inlets that are being used include parallel bar grate (P-1-7/8), parallel bar grate with transverse rods at the surface (P-1-7/8-4), parallel bar grate with spacers (P-1-1/8), 45° tilt bar grates (45-3-1/4-4, 45-2-1/4-4), 30° tilt bar grate (30-3-1/4-4), and curved vane grate (CV-3-1/4-4-1/4). **Figure 1** illustrates schematic drawings of a few grates. The flow interception capacity and hydraulic efficiency of these grates have been studied through laboratory tests by the Federal Highway Administration, and the end data was first published as design charts in the publication, referred to as HEC-12 (Hydraulic Engineering Circular No. 12) and its updated version that was revised in 2013 HEC-22 [1]. HEC-22 (Urban drainage design manual) contains information relating to the used procedures and charts to calculate the interception capacities and efficiencies of highway pavement drainage inlets for seven grate types, slotted drain inlets, curb opening inlets, and combination inlets on grade and in sump locations.

In this work, our focus is on P-1-7/8 grate. P-1-7/8-4 grate refers to a parallel bar grate with center-to-center spacing of the longitudinal bars of 48 mm (1-7/8 in). For various sump depth values, the discharge values are compared between the monograph values given in HEC-22, and the CFD model predicted data. The CFD model was developed using the popular open-source OpenFOAM[®] software. Our goal is to show that the CFD model can be reliably used to design, evaluate, and predict the efficiency of grates for different flow scenarios.

2. Review

The CFD model was developed using Open Field Operation And Manipulation (OpenFOAM[®]). OpenFOAM[®] is the leading free, open-source software for CFD, owned by OpenFOAM[®] Foundation and distributed exclusively under General Public License (GPL). It has a large user base across most areas of engineering and science, from both commercial and academic organizations. OpenFOAM[®] has an extensive range of features to solve anything from complex fluid flows involving turbulence and multi-phase, chemical reaction to acoustics, solid mechanics, and electromagnetics. Its versatile C++ toolbox for the Linux operating system enables developing customized, efficient numerical solvers and pre-/post-processing utilities for all kinds of CFD applications by solving the Navier-Stokes equations. OpenFOAM[®] uses a cell-centered Finite Volume Method (FVM) to solve the partial differential equations of continuum mechanics and fluid flow. In this approach, the equations are integrated over each of the control volumes (cells) on the mesh, and volume integrals that contain a divergence term are converted to surface integrals using Gauss's theorem. The surface integrals can then be evaluated by summing the contributions from each of the

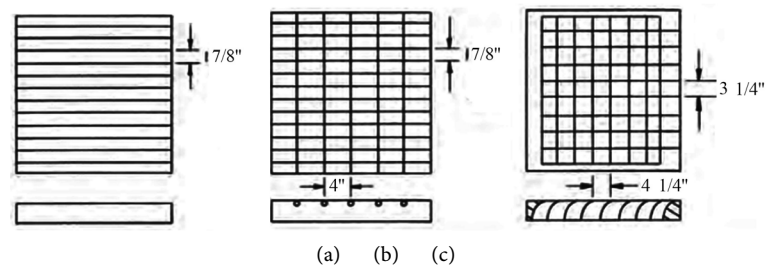


Figure 1. Schematic drawing of sample grate inlets (a) Parallel bar grate; P-1-7/8 (b) Parallel bar grate with transverse rods; P-1-7/8-4 (c) Curved vane grate; CV-3-1/4-4-1/4 [2].

cell faces. This approach to the solution of the equations requires a method to extrapolate the velocity stored at the centroid of the cell to the value of the velocity at the face of the cell. Many methods to perform this extrapolation are available in OpenFOAM, and these are documented in the Users Guide [3]. The time integration can be done through Backward Euler, Steady-state solver, Crank-Nicholson. The available gradient, divergence, Laplacian, and interpolation schemes are the second-order central difference, Fourth-order central difference, First order upwind and First/second-order upwind. OpenFOAM® provides a variety of turbulence model options from Reynolds-Averaged Navier-Stokes (RANS) to Large Eddy Simulation (LES) and Direct Numerical Simulation (DNS). The available solvers, options in specifying the boundary conditions, mesh generation tools, flow visualization software, and extensive documentation are making OpenFOAM® popular among the CFD modeling community.

3. Literature Review

The approach used for analyzing flow in grates in HEC-12 and the subsequent HEC-22 [1] monographs was based on the work on Burgi and Gober [2] who conducted comprehensive hydraulic and debris tests on eleven grate inlets to identify the grate inlets which maximize hydraulic efficiency and bicycle safety. They concluded that the hydraulic efficiency of parallel bar grate (P-1-7/8) is best until a certain longitudinal slope (S_o). Beyond this threshold slope, the efficiency falls as water starts splashing over the inlet. Since the HEC-22 was published, multiple researchers based on their experimental data, proposed changes to the equations and coefficients given in HEC-22. Guo *et al.* [4] conducted an extensive experimental study to similar real-life flow scenarios (*i.e.*, with clogging) on various grates and curb inlets and proposed different values for coefficients used in some of the equations in HEC-22. The hydraulic efficiency of grate inlets depends primarily on the street's geometry with longitudinal and transverse slope, the surface runoff (discharge) and the grate itself (type, geometry, opening area). They identified that at shallow depths, HEC-22 procedure overestimates the flow capacity of curb opening inlet. Clogging can drastically reduce the efficiency, and since debris amount varies with season and location,

they recommended a clogging factor of 0.5 for a single grate and 0.1 for a single curb-opening inlet. Muhammad [5] summarized the reported curb inlet efficiency studies and based on experimental data, proposed equations to calculate the curb opening length and inlet efficiency, for depressed inlets. The equations proposed by researchers in recent years give more reliable estimates of inlet efficiency over a broad range of input parameters, as the parameters in the equations were obtained across a higher number of physical experiments.

Galambos [6] presented experimental and numerical investigations using a 2D and 3D CFD model to better predict the flow interaction between above and below ground drainage and surcharge conditions through UK gullies. The two and three dimensional CFD model was developed using the Volume of Fluid approach on unstructured grids. The model performance was validated across 1:1 scale experimental data. The detailed CFD model provided new insights into the flow variables which cannot be measured through experiments. Their study showed that capturing many local flow parameters require using a 3D model as standard 2D models fail to reveal the physics of flow in an inlet structure. Kemper and Schlenkhoff [7] conducted physical and numerical studies to predict the efficiency of a grate inlet for supercritical flow on the grate. Their bidirectional coupled three dimensional CFD model that considers the interaction between the underground drainage system and the surface runoff used FLOW-3D software. Their focus was on evaluating the hydraulic efficiency of a typical grate inlet used in Germany (500 mm × 500 mm). They proposed an empirical formula to estimate the capacity and efficiency of the grate inlets. Since supercritical flows have upstream control, influencing parameters are water depth and velocity upstream of the grate and the grate dimensions and orientation of the bars on the surface of the grate. Fang *et al.* [8] developed a three-dimensional virtual laboratory using FLOW-3D to simulate flow at shallow depths through curb-opening inlets. Bazin *et al.* [9] developed a coupled one and two-dimensional hydrodynamic model (for pipe and street flows) and compared the predicted results with their experimental data. Other researchers who developed CFD models for analyzing flow through inlets include Djordjevic *et al.* [10] and Martins *et al.* [11] who used OpenFOAM® software to model the flow through a gully. To arrive at the efficiency of the inlet system, Shepherd *et al.* [12] measured the discharge collected by road gullies. Despotovic *et al.* [13] conducted laboratory measurements to quantify the inlet capacity and efficiency and their relationship with approaching flow, longitudinal slope, street slope, and clogging. Three dimensional CFD models, although they fail to reproduce all the flow phenomena across length and time scales, do certainly contribute to comprehend better and visualize the flow.

4. Flow Equations in HEC-22

Depending on the flow depth, the flow over the grate inlet can be either a weir flow or orifice flow. For shallow depths, the inlet operates like a weir, and for

greater or submerged depths, the inlet operates like an orifice [1]. The design chart in HEC-22 are based on the below equations

The capacity of grate inlets operating as weirs is given by (Equation 4.26 in HEC-22)

$$Q_w = C_w P d^{1.5} \quad (1)$$

where P = perimeter of the grate in ft disregarding bars and the side against the curb, d is the average depth across the grate and C_w = Coefficient of weir = 3.0.

The capacity of a grate inlet operating as an orifice is given by (Equation 4.27 in HEC-22)

$$Q_o = C_o A (2gd)^{0.5} \quad (2)$$

where C_o = orifice coefficient = 0.67; A = clear opening area of the grate = 0.9 * Area of grate, ft²; g = 32.16 ft/s².

The inlet grate capacity is minimum (Q_w , Q_o).

5. 3D Numerical Model

CFD simulation was carried out with the opensource software package OpenFOAM[®] described by Weller *et al.* [14] Numerical simulation was performed using the incompressible Navier-Stokes equations, which are derived from the first principles of conservation of mass and momentum. The continuous partial differential equations are recast into a system of linear equations. Problem closure to the Navier-Stokes equation is provided with a Newtonian relationship between stress and strain. A PISO-SIMPLE (PIMPLE, semi-implicit) algorithm was used for solving the pressure-velocity coupling. The linear equations were solved using a geometric-algebraic multigrid method (GAMG) method.

InterFoam, a Volume of Fluid (VOF) based solver, was used to compute, capture, and track the interface between air and water. The VOF method was first introduced and developed by Noh and Noh and Woodward [15], Hirt and Nichols [16]. The most widely used within practical interfacial CFD is the Volume of Fluid (VOF) method. It is a simple and flexible method for capturing and tracking the interface between two phases (air-water) using fixed mesh (no moving mesh). Also VOF only solves one set of NS equations for both phases, thus reducing the number of solved equations and computation time significantly (specifically for the models with large size/mesh and longer physical time).

The VOF method is a surface-tracking technique that models two-phase flows with a dimensionless scalar field representing the fluid volume fraction alpha (α). A volume fraction value of zero represents fluid "a," e.g., air and a value of one represents fluid "b" e.g., water. The scalar volume fraction alpha (α) is advected with the flow via a transport equation. The transport equation is solved simultaneously with the equations of mass and momentum conservation. The full set of governing equations for the fluid flow is:

$$\nabla U = 0 \quad (3)$$

$$\frac{\partial \rho u}{\partial t} + \nabla \cdot (\rho u u) - \nabla \cdot ((\mu + \mu_t) s) = -\nabla p + \rho g + \sigma K \nabla \alpha \quad (4)$$

$$\frac{\partial \alpha}{\partial t} + \nabla \cdot (u \alpha) = 0 \quad (5)$$

where u and p are velocity and pressure fields, μ_t is the turbulence eddy viscosity, s is the strain rate tensor, σ is surface tension and K is the surface curvature.

Following are the possible conditions for alpha (α):

$\alpha = 1$: volume cell occupied 100% by water.

$\alpha = 0$: volume cell occupied 100% by air.

$0 < \alpha < 1$: volume cell occupied by water and air.

Therefore the phase fraction alpha (α) must be conserved and bounded. Since the phase fraction alpha (α) can have any value between 0 and 1, the interface cannot be resolved sharply. The interface between the phases is not explicitly computed; therefore, the sharpness of the interface depends on mesh resolution around it. A sharp interface cannot be maintained if the advected term $\nabla \cdot (u \alpha)$ gets diffusive and numerical schemes do not reliably overcome the diffusion issue, therefore OpenFOAM[®] introduces a counter-diffusive term to the alpha (α) transport equation that can be used to compress the interface. The compressive convection term is presented in the third term of the transport equation below:

$$\frac{\partial \alpha}{\partial t} + \nabla \cdot (u \alpha) + \nabla \cdot (u_c \alpha (1 - \alpha)) = 0 \quad (6)$$

where u_c is the compressive velocity.

Physical properties of phases are calculated as weighted averages based on the alpha fraction. The density ρ and dynamic viscosity μ are calculated as follows:

$$\rho = \alpha \rho_{water} + (1 - \alpha) \rho_{air}$$

$$\mu = \alpha \mu_{water} + (1 - \alpha) \mu_{air}$$

6. Computational Domain

The $10 \times 5 \times 2$ m domain (**Figure 2**) was constructed with a grate in the middle. The 3D CAD of the grate was created from a schematic drawing. snappyHexMesh, an OpenFOAM mesh generation utility, was used to generate the flow domain. The snappyHexMesh utility generates 3-dimensional meshes containing hexahedra (hex cells) and split-hexahedra (split-hex) automatically from triangulated surface geometries, or ti-surfaces, in Stereolithography (STL) or Wavefront Object (OBJ) format. The flow domain was discretized, with approximately 8.0 million cells from 2 to 32 mm size ranges (**Figure 3**). Local volume regions refinement were defined to capture all geometry details in the grate. Proper surface and volume cell size distributions were applied to capture the water interface and physics precisely. Also, three prism layers were generated to capture the velocity profile at the walls. The first cell height was adjusted to gen-

erate the $Y^+ > 30$ at the walls.

The top boundary of the domain was the atmosphere, and the total pressure was set to zero. The sides of the domain were prescribed to the wall with slip conditions on velocity. The ground was segmented into two parts, one inner part around the grate and two, outer part attached to sides of the domain (**Figure 4**). The grate and part one of ground were assigned to the wall with the no-slip condition. The velocity and volume fraction were zero-gradient at the sidewalls and part one of the ground. To mimic the rainfall, the inlet was defined at the outer part of the ground. A time depended volume flow rate (**Figure 5**) was prescribed at the inlet to generate a water level on the grate from 0 to 2.2 ft. The volume fraction of $\alpha = 1$ was assigned at the inlet. Pressure outlet was assigned at the outlet of grate channel. The values of the dynamic viscosity of water and air are 0.001 Pas and 1.8 e-5 Pas, respectively. The Surface tension between air/water is 0.07 N/m.

The K-Omega SST (Reynolds Averaged Navier-Stokes type) was used as a turbulence model in this study. Gravity acceleration was activated (perpendicular to the ground) to compute the hydrostatic pressure. Wall function was used to model the near-wall conditions, where the viscous layer is not resolved explicitly, approximations are introduced to account for the flow behavior across it. Automatically adjustable time step was used based on Courant number to maintain solver stability. A transient, incompressible, and multiphase (VOF) flow was used to compute the flow fields such as velocity vector, pressure, Alpha water, turbulence properties (K, Omega) and turbulent viscosity.

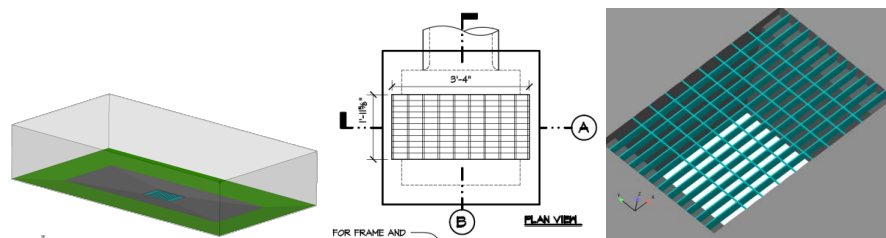


Figure 2. Schematic drawing of the grate in the flow domain.

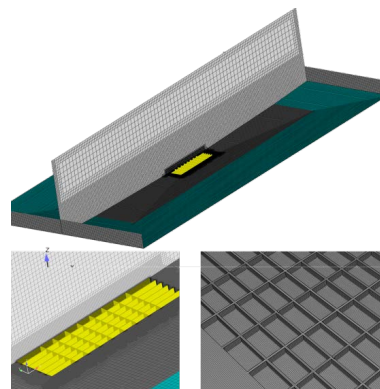


Figure 3. Discretized computational domain with approximately 8 million cells.

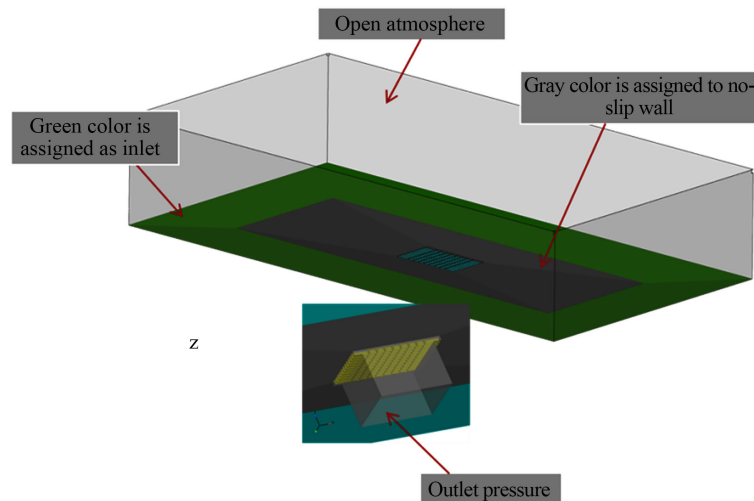


Figure 4. Computational domain with boundary conditions.

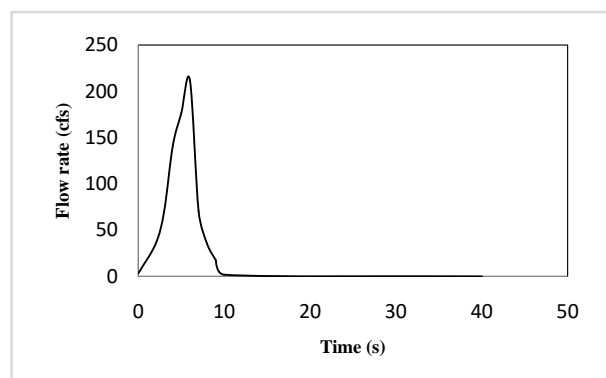


Figure 5. Inlet flow hydrograph.

7. Results

Figure 6 is a plot of the CFD predicted discharge values for flow depths ranging from 0 to 2.2 ft. The similar trend among the discharge and depth plots shows the consistency of the developed CFD model, across varying water levels. In **Figure 7**, the CFD predicted value is compared with the HEC-22 monograph value, which was obtained by solving Equations (2) and (3).

The current direction in computational hydraulic modeling advances is to resolve sets of interconnected hydraulic features into component models and develop CFD type representations of the various component sub-models, construction a system of CFD submodels. These sub modeling components are, in turn, reusable throughout the global problem domain, enabling a library of sub modeling components to be developed over time. Some civil engineering computational software products provide such reusable component CFD type models. For example, Advanced Engineering Software [17] provides base software products that readily interface with some CFD freeware and proprietary code products. These assembly submodules enable an enhanced CFD environment that will be useful in future software development products.

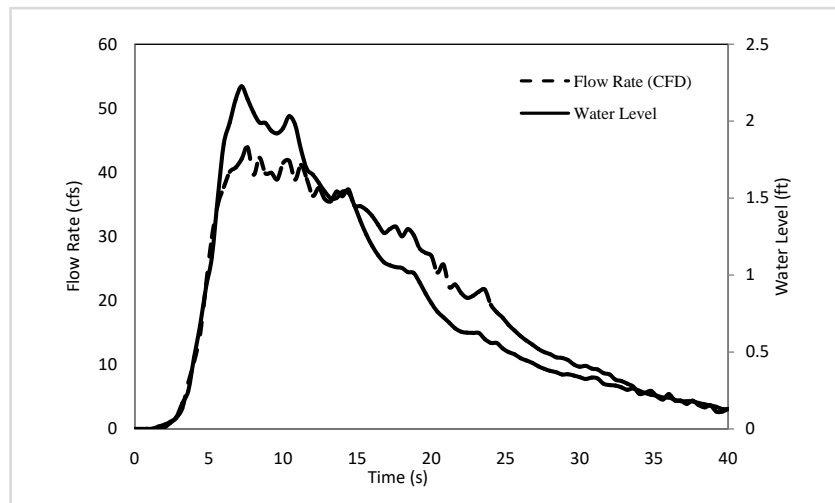


Figure 6. Variation of predicted flow rate from the CFD model across a range of water depths.

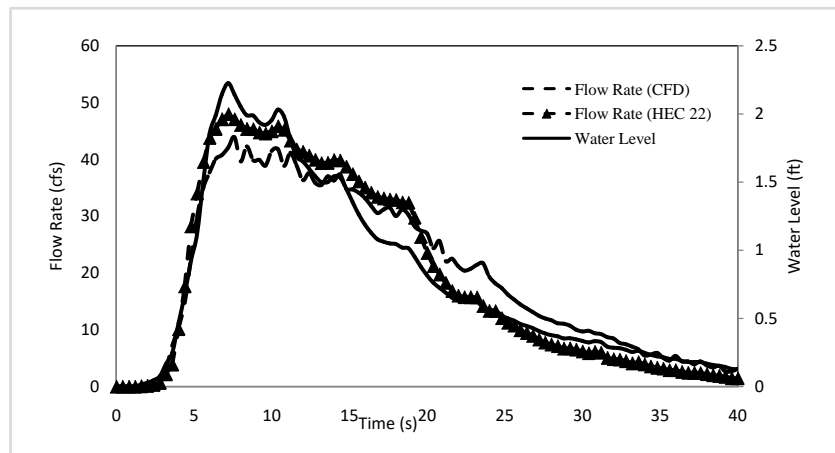


Figure 7. Plot comparing the CFD model predicted and HEC-22 flow rates for various water depths.

In the current paper, the focus is on the important submodule for drainage inlet hydraulics. Such inlets are of high population and commonly used in the design of drainage systems and in the master planning of City-wide Master Plans of Drainage. The drainage inlet submodule is the first and perhaps a fundamental component in a comprehensive CFD library of civil engineering drainage modeling elements. A library of submodules is under development and will parallel the modeling strategy used in the link-node model, such as seen in the cited Advanced Engineering Software and published in papers and texts. The close agreement of results (Figure 3) reinforces the reliability of using CFD models, which can be more accurate for many hydraulic applications.

8. Conclusion

Grated inlets are an important component of urban infrastructure, and numeri-

cal models that can predict the flow characteristics over a grate can help in simulating various flow scenarios. In this work, a three dimensional CFD model which solves the full-dimensional Navier Stokes Equations using OpenFOAM software was developed for evaluating the flow characteristics over a grate. The model results, for a range of flow depths, are compared with the HEC-22 published data. In light of the observed results, it can be concluded that the developed CFD model can be reliably used for analyzing and predicting the flow characteristics over inlet grates. Although the focus was running the model on parallel bar grate (P-1-7/8), it can be used across other grate inlets.

Conflicts of Interest

The authors declare no conflicts of interest regarding the publication of this paper.

References

- [1] Brown, S.A., Schall, J.D., Morris, J.L., Doherty, C.L., Stein, S.M. and Warner, J.C. (2013) Urban Drainage Design Manual—Hydraulic Engineering Circular 22 (HEC-22). Third Edition, U.S. Dept. of Transportation, Federal Highway Administration, Washington DC, National Highway Institute, Arlington.
- [2] Burgi, P.H. and Gober, D.E. (1978) Hydraulic and Safety Characteristics of Selected Grate Inlets. Transportation Research Record, Washington DC.
- [3] (2019) OpenFOAM: The Open Source CFD Toolbox User Guide. The Free Software Foundation Inc., Boston.
- [4] Guo, J.C.Y. and MacKenzie, K. (2012) Hydraulic Efficiency of Grate and Curb Opening Inlets under Clogging Effect. Technical Report, Colorado Department of Transportation, DTD Applied Research and Innovation Branch, 92 p.
- [5] Muhammad, M.A. (2018) Interception Capacity of Curb Opening Inlets. University of Texas at Austin, Austin.
- [6] Galambos, I. (2012) Improved Understanding of Performance of Local Controls Linking the above and below Ground Components of Urban Flood Flows. University of Exeter, Exeter.
- [7] Kemper, S. and Schlenkhoff, A. (2016) Capacity of Street Inlets with Partially Severed Grate Openings. *6th International Junior Researcher and Engineer Workshop on Hydraulic Structures*, Lübeck. <http://doi.org/10.15142/T3W01S>
- [8] Fang, X., Jiang, S. and Alam, S.R. (2010) Numerical Simulation of Efficiency of Curb-Opening Inlets. *Journal of Hydraulic Engineering*, **136**, 62-66. [https://doi.org/10.1061/\(ASCE\)HY.1943-7900.0000131](https://doi.org/10.1061/(ASCE)HY.1943-7900.0000131)
- [9] Bazin, P., Nakagawa, H., Kawaike, K., Paquier, A. and Mignot, E. (2014) Modeling Flow Exchanges between a Street and an Underground Drainage Pipe during Urban Floods. *Journal of Hydraulic Engineering*, **140**, Article ID: 04014051. [https://doi.org/10.1061/\(ASCE\)HY.1943-7900.0000917](https://doi.org/10.1061/(ASCE)HY.1943-7900.0000917)
- [10] Djordjević, S., Saul, A.J., Tabor, G.R., Blanksby, J., Galambos, I., Sabtu, N. and Sailor, G. (2013) Experimental and Numerical Investigation of Interactions between above and below Ground Drainage Systems. *Water Science and Technology*, **67**, 535-542. <https://doi.org/10.2166/wst.2012.570>
- [11] Martins, R., Leandro, J. and Carvalho, R.F. (2014) Characterization of the Hydraulic

- Performance of a Gully under Drainage Conditions. *Water Science and Technology*, **69**, 2423-2430. <https://doi.org/10.2166/wst.2014.168>
- [12] Shepherd, W., Blanksby, J., Doncaster, S. and Poole, T. (2012) Assessment of Road Gullies. *10th International Conference on Hydroinformatics*, Hamburg.
- [13] Despotovic, J., Plavsic, N., Stefanovic, N. and Pavlovic, D. (2005) Inefficiency of Storm Water Inlets as a Source of Urban Floods. *Water Science and Technology*, **51**, 139-145. <https://doi.org/10.2166/wst.2005.0041>
- [14] Weller, H., Tabor, G., Jasak, H. and Fureby, C. (1988) Tensorial Approach to Computational Continuum Mechanics Using Object-Oriented Techniques. *Computers in Physics*, **12**, 620-631. <https://doi.org/10.1063/1.168744>
- [15] Noh, W.F. and Woodward, P. (1976) SLIC (Simple Line Interface Calculation). In: van Dooren, A.I. and Zandbergen, P.J., Eds., *Lecture Notes in Physics*, Springer, Berlin, Vol. 59, 330-340.
- [16] Hirt, C.W. and Nichols, B.D. (1981) Volume of Fluid (VOF) Method for the Dynamics of Free Boundaries. *Journal of Computational Physics*, **39**, 201-225. [https://doi.org/10.1016/0021-9991\(81\)90145-5](https://doi.org/10.1016/0021-9991(81)90145-5)
- [17] Advanced Engineering Software, Engineering Hydrologic Software Solutions. <http://advancedengineeringsoftware.com>